Impaired vascular remodeling in yolk sac of embryos deficient in ROCK-I and ROCK-II

Running Title; DEVELOPMENTAL DEFECTS OF ROCK-DEFICIENT MICE

Hiroshi Kamijo, Yutaka Matsumura, Dean Thumkeo, Yoshihiko Shimizu, Toshimasa Ishizaki, and Shuh Narumiya

Department of Pharmacology, Kyoto University Faculty of Medicine, Kyoto 606-8501, Japan

Correspondence to Shuh Narumiya: snaru@mfour.med.kyoto-u.ac.jp

FAX: 81-75-753-4693

Abbreviations used in this paper: MLC, myosin light chain; ROCK, Rho-associated kinase MYPT: myosin phosphatase PECAM: platelet endothelial cell adhesion molecule

Abstract

Rho-associated coiled-coil-forming protein serine／threonine kinase (ROCK) consisting of two isoforms, ROCK-I and ROCK-II, functions downstream of the small GTPase Rho for assembly of actomyosin bundles. To examine the role of ROCK isoforms *in vivo*, we previously generated and examined mice deficient in each of the two isoforms individually. Here, we further examined the *in vivo* role of ROCK isoforms by generating mice deficient in both isoforms. Cross-mating of ROCK-I$^{+/-}$ROCK-II$^{+/-}$ double heterozygous mice showed that all of the ROCK-I$^{-/-}$ROCK-II$^{-/-}$ homozygous mice die in utero before 9.5 days post-coitum (dpc) and ROCK-I$^{-/-}$ROCK-II$^{+/-}$ homo-heterozygous or ROCK-I$^{+/-}$ROCK-II$^{-/-}$ hetero-homozygous mice die during a period from 9.5 to 12.5 dpc, whereas mice of other genotypes survive until 12.5 dpc with the expected Mendelian ratio. All of the ROCK-I$^{+/-}$ROCK-II$^{-/-}$ or ROCK-I$^{-/-}$ROCK-II$^{+/-}$ mice showed impaired body turning and defective vascular remodeling in the yolk sac. Impairment of vascular remodeling was also observed in wild-type embryos treated ex vivo with a ROCK inhibitor, Y-27632. These results suggest that ROCK isoforms function redundantly during embryogenesis and play a critical role in vascular development.

Introduction

Rho-associated coiled-coil-forming protein serine/threonine kinase (ROCK) is an effector of the small GTPase Rho and functions in various Rho-mediated cellular processes including stress fiber formation, cell adhesion, migration, phagocytosis, apoptotic cell blebbing, neurite retraction, malignant transformation, cancer cell invasion, smooth muscle contraction, and cytokinesis (Riento & Ridley 2003) Most of these ROCK actions are exerted by spatiotemporal induction and contraction of actomyosin bundles in a manner dependent on the context of a cell through phosphorylation of MLC. ROCK activates myosin by either inhibiting myosin phosphatase (MYPT) or directly phosphorylating myosin light chain (MLC) (Kimura *et al.* 1996). ROCK also inhibits depolymerization of actin filaments by inhibiting coffilin/ADF through activation of LIM kinase (Maekawa *et al.* 1999).

Although in vivo relevance of some of these findings have been examined by the use of ROCK-specific inhibitors such as Y-27632 (Uehata *et al.* 1997), what actions ROCK exerts in the body, especially during development, and how critical these ROCK actions are remain largely unknown. ROCK consists of two isoforms, ROCK-I and ROCK-II. To address the above issue, we previously generated mice deficient in each of the ROCK isoforms individually, and examined their phenotypes. We found the

eyes-open-at-birth (EOB) phenotype and omphalocele in neonates deficient in either ROCK-I or ROCK-II (Shimizu *et al.* 2005; Thumkeo *et al.* 2005). In these mice, the actomyosin bundles encircling the eyelid were severely disorganized, and accumulation of phosphorylated MLC at the epidermal ridge of the umbilical region was greatly attenuated, indicating that such failure of the body wall closure in these mice is due to impaired formation of the ROCK-catalyzed actomyosin-based constriction machinery in the tissues. In addition to the above defect, the ROCK-II deficiency also caused thrombus formation in the placenta and led to intrauterine growth retardation and fetal death due to placental dysfunction (Thumkeo *et al.* 2003). ROCK-I and ROCK-II show the same domain structure with more than 65% amino acid sequence homology in their entire sequence (Nakagawa *et al.* 1996) and their tissue expression patterns partially overlap. Reflecting a functional redundancy of ROCK-I and ROCCK-II, ROCK-I$^{+/-}$ROCK-II$^{+/-}$ embryos also showed the EOB phenotype as ROCK-I or ROCK-II deficient mice (Thumkeo *et al.* 2005).

Given possible redundant role of the two ROCK isoforms in embryogenesis, here we have intercrossed ROCK-I$^{+/-}$ROCK-II$^{+/-}$ double heterozygous mice and generated mice null of both ROCK isoforms or containing only a single allele of one isoform, and examined their phenotypes.

Results

Generation of ROCK-I and ROCK-II double deficient mice

To examine the role of ROCK-I and ROCK-II in embryonic development, we intercrossed ROCK-I$^{+/-}$ROCK-II$^{+/-}$ double-heterozygous (DHT) mice, and analyzed genotype distribution in the offspring. Genotype analysis of 136 offspring obtained at 9.5 dpc revealed that no ROCK-I/ROCK-II null (ROCK-I$^{-/-}$ROCK-II$^{-/-}$) embryos were obtained at this stage. The number of ROCK-I$^{+/-}$ROCK-II$^{-/-}$, ROCK-I$^{-/-}$ROCK-II$^{+/+}$ and ROCK-I$^{-/-}$ROCK-II$^{+/-}$ embryos was less than that expected from the Mendelian ratio in this experiment and that of offsprings of other genotypes, which followed the Mendelian ratio (Table 1). Further analysis of embryos at 12.5 dpc revealed that in addition to ROCK-I/ROCK-II null embryos, no ROCK-I$^{-/-}$ROCK-II$^{+/-}$ and ROCK-I$^{+/-}$ROCK-II$^{-/-}$ embryos were obtained at this stage. We then performed in vitro fertilization (IVF) and found that ROCK-I/ROCK-II null embryos were present at the expected Mendelian frequency at 3.5 dpc (Table 2). Thus, the loss of both alleles resulted in lethality of embryos from 3.5 to 9.5 dpc, and the insufficiency of ROCK isoforms impaired mouse development during a period from 9.5 to 12.5 dpc. These results indicate that ROCK-I and ROCK-II play redundant and essential roles during mouse development.

Morphology of ROCK-I$^{-/-}$ROCK-II$^{+/-}$ and ROCK-I$^{+/-}$ROCK-II$^{-/-}$ embryos

We next characterized developmental defects of ROCK-I$^{-/-}$ROCK-II$^{+/-}$ and ROCK-I$^{+/-}$ROCK-II$^{-/-}$ embryos between 9.5 and 12.5 dpc. To obtain an enough number of ROCK-I$^{-/-}$ROCK-II$^{+/-}$ and ROCK-I$^{+/-}$ROCK-II$^{-/-}$ embryos, we crossed DHT mice with either ROCK-I$^{+/-}$ROCK-II$^{+/+}$ or ROCK-I$^{+/+}$ROCK-II$^{+/-}$ mice. Offspring obtained from these mating procedures also followed the Mendelian ratio at 9.5 dpc (data not shown). We found all ROCK-I$^{-/-}$ROCK-II$^{+/-}$ and ROCK-I$^{+/-}$ROCK-II$^{-/-}$ embryos examined at this stage (9 and 12, respectively) did not show body turning (Fig. 1D, G), while other embryos completed body turning at this stage (Fig. 1A).

All of the ROCK-I$^{-/-}$ROCK-II$^{+/-}$ and ROCK-I$^{+/-}$ROCK-II$^{-/-}$ embryos at 9.5 dpc were smaller than that of wild type embryos of the same stage and of about the same size as that of 8.5 dpc wild type embryos (Fig. 1A, D and G). The number of somites in ROCK-I$^{-/-}$ROCK-II$^{+/-}$ and ROCK-I$^{+/-}$ROCK-II$^{-/-}$ embryos at this stage was 10-14, significantly small compared to the other genotypes (18-25 somites) (Fig. 1J) and comparable to 8.5 dpc wild type embryos (around 10 somites). These results suggest that ROCK deficiency retards the growth of embryos at this stage.

Inspection of the yolk sac revealed that, while the blood apparently filled the tree-like hierarchical structure consisting of larger and smaller vessels in wild type yolk sac at

9.5 dpc (Fig. 1B, C), the blood was pooled in irregular sinusoid-like structure in yolk sacs of ROCK-I$^{-/-}$ROCK-II$^{+/-}$ and ROCK-I$^{+/-}$ROCK-II$^{-/-}$ embryos (Fig. 1E, F, H and I). This yolk sac phenotype was always associated with impaired body turning in embryos of this genotype. Immunoblot analysis with antibodies to ROCK-I and ROCK-II revealed that both ROCK-I and ROCK-II were detected in lysates of embryonic proper as well as the yolk sac at 9.5 dpc (Fig. 2A). Given that a lacZ reporter gene was knocked-in in-frame with the initiator methionine of ROCK-I and ROCK-II in individual ROCK-I and ROCK-II targeting constructs (Thumukeo *et al* 2003, Shimizu *et al* 2005), we next performed whole-mount β-galactosidase staining in yolk sac of ROCK-I$^{-/-}$ROCK-II$^{+/+}$ and ROCK-I$^{+/+}$ROCK-II$^{-/-}$ embryos at 9.5 dpc. The staining for ROCK-I and ROCK-II was observed along the blood vessels in the yolk sac, and the cross section revealed that they were preferentially expressed in endothelial cells (Fig. 2B).

Defective vasculogenesis in ROCK-mutant embryos

To characterize the abnormality in the yolk sac of ROCK-mutant embryos, we performed whole mount staining with antibody to Flk-1 (also named VEGFR-2 or KDR) as a maker of primitive endothelial cells. Flk-1-positive signals were observed in the yolk sac of ROCK-I$^{-/-}$ROCK-II$^{+/-}$ and ROCK-I$^{+/-}$ROCK-II$^{-/-}$ embryos, as well as

embryos of other genotypes, indicating that vascular endothelial cells were differentiated and present in the ROCK-I$^{-/-}$ROCK-II$^{+/-}$ and ROCK-I$^{+/-}$ROCKII$^{-/-}$ embryos (Fig. 3A, B, D and E).. However, while the vasculature of the WT yolk sac was composed of the meshwork of vessels of similar calibers at 8.5 dpc, and remodeled to resemble a mature system of large and small vessels at 9.5 dpc (Fig. 3 A and B), Flk-1-positive signals covered continuously over the yolk sac with occasional, irregular sized holes, making meshwork-like structure in some areas, in ROCK-I$^{-/-}$ROCKII$^{+/-}$ and ROCK-I$^{+/-}$ROCK-II$^{-/-}$ embryos at 9.5 dpc (Fig. 3D, E). Cross-sections of these preparations clearly showed that, whereas the vessels of various calibers were formed in the wild-type yolk sac at 9.5 dpc (Fig. 3C), the vascular lumen was widely open and extended laterally between the visceral endoderm and mesoderm layers in the yolk sac of ROCK-I$^{-/-}$ROCK-II$^{+/-}$ and ROCK-I$^{+/-}$ROCKII$^{-/-}$ embryos (Fig. 3F, G). Platelet endothelial cell adhesion molecule-1 (PECAM-1), a marker for definitive embryonic endothelial cells, had a staining pattern similar to that of Flk-1 (data not shown). Despite this vascular defect, erythrocytes were present in the yolk sac in ROCK-I$^{-/-}$ROCK-II$^{+/-}$ and ROCK-I$^{+/-}$ROCK-II$^{-/-}$ embryos (Fig. 3F, G). These results taken together show that although endothelial cells were present in ROCK-I$^{-/-}$ROCK-II$^{+/-}$ and ROCK-I$^{+/-}$ROCK-II$^{-/-}$ yolk sac, they failed to form tubular

structures.

Activity of ROCK is required for vascular remodeling in the yolk sac during embryogenesis

To examine whether the kinase activity of ROCK is required for vascular remodeling in the yolk sac, we carried out an ex vivo whole-embryo culture in the presence of 1 and 3 μM of Y-27632, a selective ROCK inhibitor, and analyzed the morphology of embryos. When 7.5 dpc wild-type embryos were cultured for 1 and 2 days in the absence of Y-27632, they developed with a normal appearance comparable to those of in utero-grown 8.5 and 9.5 dpc embryos, respectively (Fig. 4A, D; data not shown). Vascular remodeling and body turning were observed at 48 h (Fig. 4A, D). The appearance of the embryos and yolk sacs in the presence of Y-27632 of both concentrations was similar up to 24 h to that of those cultured in the absence of Y-27632 (data not shown). However, after 48 h, embryos treated with Y-27632 showed impaired body turning and a vascular defect in the yolk sac (Fig. 4B, C, E and F), as seen in ROCK-I$^{+/-}$ROCK-II$^{-/-}$ and ROCK-I$^{-/-}$ROCKII$^{+/-}$ embryos (Fig. 1D–I). Impairment of vascular remodeling was milder in embryos treated with 1 μM Y-27632 than that with 3 μM of the inhibitor (Fig. 4B, C). Consistently, hematoxylin–eosin staining of cryosections showed the widely open vascular lumen in the yolk sac treated with both

concentrations of Y-27632, which is very similar to those found in ROCK-I$^{+/-}$ROCK-II$^{-/-}$ and ROCK-I$^{-/-}$ROCKII$^{+/-}$ embryos. This phenotype was again milder in the yolk sac treated with 1 μM Y-27632 (Fig. 4H, I). These results suggest that the kinase activity of ROCK is required for vascular remodeling between 8.5 and 9.5 dpc. To verify that ROCK actually exerted the kinase activity in situ in the yolk sac of this stage, we examined the in vivo phosphorylation level of MLC and MYPT, two endogenous substrates of ROCK. We harvested ROCK-I$^{+/-}$ROCK-II$^{-/-}$ and ROCK-I$^{-/-}$ROCKII$^{+/-}$ embryos at 9.5 dpc as well as embryos after 48 h culture in the presence or absence of different concentrations of Y-27632. The yolk sacs were isolated, subjected to SDS-PAGE and analyzed by immunoblotting with antibodies to phospho-MYPT and phospho-MLC (Fig. 5). Immunoblotting analysis showed a decrease in MYPT and MLC phosphorylation in the yolk sac obtained from ROCK-I$^{+/-}$ROCK-II$^{-/-}$ and ROCK-I$^{-/-}$ROCKII$^{+/-}$ embryos at 9.5 dpc compared to that in wild-type yolk sac. It further showed that phosphorylation of MYPT in the yolk sac was concentration dependently decreased by the Y-27632 treatment, while MLC phosphorylation was almost completely suppressed by treatment even with 1 μM Y-27632.

Discussion

In this study, we have found that ROCK-I/ROCK-II null (ROCK-$I^{-/-}$ROCK-$II^{-/-}$) embryos die between 3.5 and 9.5 dpc, and that both ROCK-$I^{-/-}$ROCK-$II^{+/-}$ and ROCK-$I^{+/-}$ROCK-$II^{-/-}$ embryos die between 9.5 dpc and 12.5 dpc. Furthermore, we have observed that both ROCK-$I^{-/-}$ROCK-$II^{+/-}$ and ROCK-$I^{+/-}$ROCK-$II^{-/-}$ embryos show severe impairment of vascular development in yolk sacs and growth retardation at 9.5 dpc and the vascular lumens in the yolk sacs of these embryos are widely open. These phenotypes were mimicked by culture of embryos ex vivo in the presence of Y-27632. Notably the phosphorylation level of MLC and MYPT, endogenous substrates for ROCK, is decreased in both ROCK-$I^{-/-}$ROCK-$II^{+/-}$ and ROCK-$I^{+/-}$ROCK-$II^{-/-}$ embryos at 9.5 dpc as well as Y-27632 treated-embryos. Taken together, these results suggest that ROCK isoforms function redundantly and are required for embryonic development at different developmental stages during early embryogenesis.

During mammalian development, *de novo* blood vessel formation initially occurs extraembryonically within the mesodermal layer of the yolk sac. Mesodermal progenitors cluster at sites of blood vessel formation and undergo differentiation into endothelial and blood cells, forming blood islands (Ferkowicz & Yoder 2005). Endothelial cells then migrate and re-align to form tubular structures that fuse to create

an interconnecting network of vessels referred to as the primitive capillary plexus. Remodeling of the capillary plexus into a functional hierarchical network of large, medium, and small diameter vessels are carried out by proliferation of endothelial cells, their sprouting, intussusception and then a process called pruning (Risau 1997; Lamalice *et al.* 2007). As the erythrocytes and endothelial cells are both present in the mutant yolk sac, and the latter form the lumen, it appeared that the differentiation of haemangioblasts to hematopoietic stem cells and angioblasts occurs and resultant endothelial cells migrate from blood islands and fuse each other also in the mutant yolk sac. However, the lumen formed in ROCK-$I^{-/-}$ROCK-$II^{+/-}$ and ROCK-$I^{+/-}$ROCK-$II^{-/-}$ yolk sac is mostly widely open sinusoid-like structure, although the capillary plexus-like appearance was seen in some areas. This phenotype is mimicked by pharmacological inhibition of ROCK with Y-27632. These results suggest that the ROCK activity is required for initial capillary tube formation and／or maintenance or later sprouting and intussusception that refine vascular network or both. Sprouting and intussusception are angiogenesis processes that occur in the preexisting blood vessels, and our findings may be consistent with the findings by Hoang *et al.* (2004) that Rho activity is required for VEGF-regulated angiogenesis and that both Rho and ROCK activities are required for formation of the multicellular, pre-capillary cord-like structure

by endothelial cells on the collage-I gel culture. The formation of the latter structure requires ROCK-mediated endothelial cell contraction of collagen gels. Notably, significant decrease in MLC phosphorylation was found in the yolk sac of ROCK-$I^{-/-}$ROCKII$^{+/-}$ and ROCK-$I^{+/-}$ROCK-$II^{-/-}$ embryos or embryos treated with Y-27632 *ex vivo*, suggesting that actomyosin contraction in this tissue is mainly exerted by the Rho-ROCK pathway at this stage. Given that both ROCK isoforms are expressed in endothelial cells in the yolk sac at this stage, ROCK-exerted actomyosin contractility appears to contribute to endothelial functions at this time of vasculogenesis. In addition to impaired vessel formation in the yolk sac, we observed impaired body turning in ROCK-$I^{-/-}$ROCK-$II^{+/-}$ and ROCK-$I^{+/-}$ROCK-$II^{-/-}$ embryos, and these two phenotypes accompany each other. In this study we could not determine whether these two are of causative relation or induced by separate mechanisms both due to ROCK insufficiency. However, the vascular defect in the yolk sac can be a cause of developmental delay, because proper circulation can be maintained by the mature hierarchical vessel system. Indeed, the blood did not appear to circulate properly in the yolk sac of ROCK-$I^{-/-}$ROCK-$II^{+/-}$ and ROCK-$I^{+/-}$ROCK-$II^{-/-}$ embryos compared to that of wild type embryos (data not shown).

Vascular remodeling is regulated by a variety of factors including various

angiogenic factors, local mediators, extracellular matrix and shear stress (Carmeliet 2000). Shear stress exerted by the blood flow on the endothelium is important for vascular remodeling *in vivo* (Chiu & Chien 2011). *In vitro* experiments have demonstrated that shear stress selectively promotes the differentiation of Flk-1^+ ES cells into the endothelial cell lineage and the shear stressed Flk-1^+ ES cells could form tube-like structures in collagen gel and developed extensive tubular networks (Yamamoto *et al.* 2005). Interestingly, shear stress induces and orients actin stress fibers in endothelial cells both in vivo (Davies *et al.* 1994) and in vitro (van der Meer *et al.*; Wojciak-Stothard & Ridley 2003), and that this induction depends on the Rho-ROCK pathway (Li *et al.* 1999; Birukov *et al.* 2002). These results suggest a possibility that ROCK functions as a mechano-transducer to shear stress to induce vascular remodeling through actomyosin contractility. Finally, similar vascular defect and impaired body turning we observed here in ROCK-$I^{-/-}$ROCK-$II^{+/-}$ and ROCK-$I^{+/-}$ROCK-$II^{-/-}$ embryos were reported in mice deficient in autoaxin (ATX) and $G\alpha_{13}$ (Offermanns *et al.* 1997; Ruppel *et al.* 2005; Tanaka *et al.* 2006; van Meeteren *et al.* 2006). Autoaxin belongs to the nucleotide pyrophosphatase (NPP) family of ectoenzyme and exoenzyme. This enzyme converts lysophosphatidylcholine (LPC) into bioactive lysophosphatidic acid (LPA). LPA is known as a strong inducer of acitn

stress fibers in cultured fibroblasts and acts on a family of G protein-coupled receptors. Signaling from LPA receptor to Rho activation is mediated by $G\alpha_{12/13}$ and p115 Rho guanine exchange factor. Thus, it is tempting to speculate that a pathway defined to control stress fiber formation in cultured cells is involved in vascular remodeling, although this pathway functions in endothelial cells in the yolk sac remains to be elucidated.

Experimental procedures

Mice

Generation of ROCK-I and ROCK-II KO mice have been described previously (Thumkeo *et al*. 2003, Shimizu *et al*. 2005). Double heterozygous (ROCK-$I^{+/-}$ROCK-$II^{+/-}$) mice were generated by cross-mating of ROCK-$I^{+/+}$ROCK-$II^{+/-}$ mice with ROCK-$I^{+/-}$ROCK-$II^{+/+}$ mice. The morning of the day on which a vaginal plug was detected was designated as 0.5 dpc. All animal experiments were approved by the Committee on Animal Research of Kyoto University Faculty of Medicine and were performed according to the guidelines for the protection of experimental animals of Kyoto University.

Antibodies

Rat polyclonal anti-Flk-1 antibody and rat polyclonal anti-PECAM-1 antibody were purchased from BD bioscience. Rabbit polyclonal anti-ROCK-I (H-85) antibody and rabbit polyclonal anti-ROCK-II (H85) antibody were purchased from Santa Cruz. Rabbit polyclonal phospho-MLC antibody, rabbit polyclonal phospho-MYPT antibody and mouse monoclonal β-Actin antibody were purchased from Cell signaling, Millipore and Sigma, respectively.

Immunohistochemistry and β-gal staining

The embryos were fixed in PBS containing 4 % paraformaldehyde for 15 min at room temperature (RT), and replaced in 30% sucrose and embedded in OCT compound (Sakura Finetek). The embedded embryos were sectioned with 10 μm thickness. After washing with PBS, the specimens were incubated with primary antibodies, Flk-1(1:250) or PECAM-1(1:250) diluted in PBS containing 1 % skim milk, and then incubated with biotin-conjugated anti-rat IgG. The specimens were stained using the avidin-biotinylated peroxidase complex (Vectostain ABC-Kit, Vector Lab) and substrate solution 3,3-diamino-benzidine (DAB, Vector Lab). For β-gal staining, the embryos were fixed in PBS containing 0.2% glutaraldehyde, 5 mM EGTA and 2 mM $MgCl_2$ and stained with X-gal (Thumkeo et al 2002). For histological examination, the sections were stained with hematoxylin and eosin (HE).

Immunoblotting

For the experiment in Fig. 2A, the embryonic bodies and yolk sacs were obtained from the wild type embryos dissected at 9.5 dpc. For the experiment in Fig. 5, the yolk sacs were obtained from either the wild type embryos cultured for 48 h in the presence or absence of Y-27632 or the indicated genotypic embryos. The yolk sacs and bodies were lysed with laemmli buffer. The lysates were subjected to SDS-PAGE and

analyzed by immunoblotting with antibodies to either ROCK-I, ROCK-II, phospho-MLC (p-MLC), phospho-MYPT (p-MYPT) or β-Actin.

Microscopy

The photos of whole-mount views of freshly dissected embryos with or without intact yolk sacs were taken by SVZ-61(Olympus). The image of specimens stained with anti-Flk-1 antibody and HE were taken by DP-70 (Olympus) equipped with CCD-camera.

Whole embryo culture

Embryos were dissected at 7.5 dpc form C57B6/N and cultured in 100 % rat serum (Charles River) supplemented with 2 mg/ml glucose in a culture bottle placed in a rotation drum culture system (Ikemoto Rika) and with or without 3 μM Y-27632 at 37 ^{o}C under 5 % O_2, 5 % CO_2, and 90 % N_2 for the initial 24 h, followed by 20 % O_2, 5 % CO_2, and 75 % N_2 for the next 24 h.

References

Aoki, J. (2004) Mechanisms of lysophosphatidic acid production. *Semin. Cell Dev. Biol.*15, 477–489.

Carmeliet, P. (2000) Mechanisms of angiogenesis and arteriogenesis. *Nat. Med.* 6, 389–395.

Chiu, J.J. & Chien, S. (2011) Effects of disturbed flow on vascular endothelium: pathophysiological basis and clinical perspectives. *Physiol. Rev.* 91, 327–387.

Davies, P.F., Robotewskyj, A. & Griem, M.L. (1994) Quantitative studies of endothelial cell adhesion. Directional remodeling of focal adhesion sites in response to flow forces. *J. Clin. Invest.* 93, 2031–2038.

Ferkowicz, M.J. & Yoder, M.C. (2005) Blood island formation: longstanding observations and modern interpretations. *Exp. Hematol.* 33, 1041–1047.

Hoang, M.V., Whelan, M.C. & Senger, D.R. (2004) Rho activity critically and selectively regulates endothelial cell organization during angiogenesis. *Proc. Natl Acad. Sci.* USA. 101, 1874–1879.

Kimura, K., Ito, M., Amano, M., Chihara, K., Fukata, Y., Nakafuku, M., Yamamori, B., Feng, J., Nakano, T., Okawa, K., Iwamatsu, A. & Kaibuchi, K. (1996) Regulation of myosin phosphatase by Rho and Rho-associated kinase (Rho-kinase). *Science*

273, 245–248.

Koike, S., Keino-Masu, K. & Masu, M. (2010) Deficiency of autotaxin / lysophospholipase D results in head cavity formation in mouse embryos through the LPA receptor- Rho-ROCK pathway. *Biochem. Biophys. Res. Commun.* 400,66–71.

Kozasa, T., Jiang, X., Hart, M.J., Sternweis, P.M., Singer, W.D., Gilman, A.G., Bollag, G. & Sternweis, P.C. (1998) p115 RhoGEF, a GTPase activating protein for Galpha12 and Galpha13. Science 280, 2109–2111.

Lamalice, L., Le Boeuf, F. & Huot, J. (2007) Endothelial cell migration during angiogenesis. *Circ. Res.* 100, 782–794.

Li, S., Chen, B.P., Azuma, N., Hu, Y.L., Wu, S.Z., Sumpio, B.E., Shyy, J.Y. & Chien, S. (1999) Distinct roles for the small GTPases Cdc42 and Rho in endothelial responses to shear stress. J. Clin. Invest. 103, 1141–1150.

Maekawa, M., Ishizaki, T., Boku, S., Watanabe, N., Fujita, A., Iwamatsu, A., Obinata, T., Ohashi, K., Mizuno, K. & Narumiya, S. (1999) Signaling from Rho to the actin cytoskeleton through protein kinases ROCK and LIM-kinase. *Science* 285, 895–898.

van der Meer, A.D., Poot, A.A., Feijen, J. & Vermes, I. (2010) Analyzing shear

stress-induced alignment of actin filaments in endothelial cells with a microfluidic assay. *Biomicrofluidics* 4, 11103.

van Meeteren, L.A., Ruurs, P., Stortelers, C., Bouwman, P., van Rooijen, M.A., Pradere, J.P., Pettit, T.R., Wakelam, M.J., Saulnier-Blache, J.S., Mummery, C.L., Moolenaar, W.H. & Jonkers, J. (2006) Autotaxin, a secreted lysophospholipase D, is essential for blood vessel formation during development. *Mol. Cell. Biol.* 26, 5015–5022.

Moolenaar, W.H., Kranenburg, O., Postma, F.R. & Zondag, G.C. (1997) Lysophosphatidic acid: G-protein signalling and cellular responses. *Curr. Opin. Cell Biol.* 9, 168–173.

Nakagawa, O., Fujisawa, K., Ishizaki, T., Saito, Y., Nakao, K. & Narumiya, S. (1996) ROCK-I and ROCK-II, twoisoforms of Rho-associated coiled-coil forming protein serine/threonine kinase in mice. *FEBS Lett.* 392, 189–193.

Offermanns, S., Mancino, V., Revel, J.P. & Simon, M.I. (1997) Vascular system defects and impaired cell chemokinesis as a result of Galpha 13 deficiency. *Science* 275, 533–536.

Osumi-Yamashita, N., Ninomiya, Y. & Eto, K. (1997) Mammalian craniofacial embryology in vitro. *Int. J. Dev. Biol.* 41, 187–194.

Riento, K. & Ridley, A.J. (2003) Rocks: multifunctional kinases in cell behaviour. *Nat. Rev. Mol. Cell Biol.* 4, 446–456.

Risau, W. (1997) Mechanisms of angiogenesis. *Nature* 386, 671–674.

Ruppel, K.M., Willison, D., Kataoka, H., Wang, A., Zheng, Y.W., Cornelissen, I., Yin, L., Xu, S.M. & Coughlin, S.R. (2005) Essential role for Galpha13 in endothelial cells during embryonic development. *Proc. Natl Acad. Sci.* USA. 102, 8281–8286.

Shimizu, Y., Thumkeo, D., Keel, J., Ishizaki, T., Oshima, H., Oshima, M., Noda, Y., Matsumura, F., Taketo, M.M. & Narumiya, S. (2005) ROCK-I regulates closure of the eyelids and ventral body wall by inducing assembly of actomyosin bundles. *J. Cell Biol.* 168, 941–953.

Tanaka, M., Okudaira, S., Kishi, Y., Ohkawa, R., Iseki, S., Ota, M., Noji, S., Yatomi, Y., Aoki, J. & Arai, H. (2006) Autotaxin stabilizes blood vessels and is required for embryonic vasculature by producing lysophosphatidic acid. *J. Biol. Chem.* 281, 25822–25830.

Thumkeo, D., Keel, J., Ishizaki, T., Hirose, M., Nonomura, K., Oshima, H., Oshima, M., Taketo, M.M. & Narumiya, S. (2003) Targeted disruption of the mouse rho-associated kinase 2 gene results in intrauterine growth retardation and fetal death. *Mol. Cell. Biol.* 23, 5043–5055.

Thumkeo, D., Shimizu, Y., Sakamoto, S., Yamada, S. & Narumiya, S. (2005) ROCK-I and ROCK-II cooperatively regulate closure of eyelid and ventral body wall in mouse embryo. *Genes Cells* 10, 825–834.

Tokumura, A., Harada, K., Fukuzawa, K. & Tsukatani, H. (1986) Involvement of lysophospholipase D in the production of lysophosphatidic acid in rat plasma. *Biochim. Biophys. Acta.* 875, 31–38.

Uehata, M., Ishizaki, T., Satoh, H., Ono, T., Kawahara, T., Morishita, T., Tamakawa, H., Yamagami, K., Inui, J., Maekawa, M. & Narumiya, S. (1997) Calcium sensitization of smooth muscle mediated by a Rho-associated protein kinase in hypertension. *Nature* 389, 990–994.

Wojciak-Stothard, B. & Ridley, A.J. (2003) Shear stressinduced endothelial cell polarization is mediated by Rho and Rac but not Cdc42 or PI 3-kinases. *J. Cell Biol.* 161, 429–439.

Yamamoto, K., Sokabe, T., Watabe, T., Miyazono, K., Yamashita, J.K., Obi, S., Ohura, N., Matsushita, A., Kamiya, A. & Ando, J. (2005) Fluid shear stress induces differentiation of Flk-1-positive embryonic stem cells into vascular endothelial cells in vitro. *Am. J. Physiol. Heart Circ. Physiol.* 288, H1915–H1924.

Figure legends

Figure 1 Phenotypes of ROCK-I$^{+/-}$ROCK-II$^{-/-}$ and ROCK-I$^{-/-}$ROCK-II$^{+/-}$ embryos at 9.5 dpc.

Photographs of freshly dissected ROCK-I$^{+/+}$ROCK-II$^{+/-}$, ROCK-I$^{-/-}$ROCK-II$^{+/-}$ and ROCK-I$^{+/-}$ROCK-II$^{-/-}$ embryos with (B, E and H) or without intact yolk sacs (A, D and G). C, F and I show the higher magnification images of boxed areas in B, E and H, respectively. Bars, 500 μm. (J) The number of somites in the embryos at 9.5 dpc. *** denotes $P < 0.001$(Student's t-test).

Figure 2 ROCK-I and ROCK-II are expressed in 9.5 dpc embryos.

(A) Wild-type embryos were collected at 9.5 dpc. Embryonic bodies and yolk sacs were separated and lysed with Laemmli buffer, subjected to SDS-PAGE and then analyzed by immunoblotting with antibodies to ROCK-I (an upper panel) and ROCK-II (a lower panel). Note that both ROCK-I and ROCK-II were expressed in the embryonic body and the yolk sac at this stage. (B) Whole-mount X-gal staining. ROCKI$^{-/-}$ROCK-II$^{+/+}$ (upper left panel) and ROCK-I$^{+/+}$ROCKII$^{-/-}$ (upper right panel) embryos were collected at 9.5 dpc and were performed X-gal staining as described in Experimental procedures. Bars, 250 μm. Slices sectioned along the transverse plane of X-gal-stained ROCK-I$^{-/-}$ROCK-II$^{+/+}$ (bottom left panel) and ROCK-I$^{+/+}$ROCK-II$^{-/-}$ (bottom right

panel) embryo yolk sacs were shown (bottom panels). Bars, 25 μm. Note that both ROCK-I and ROCK-II are expressed in the yolk sac along the vasculature, especially in endothelial cells.

Figure 3 Defective vascular remodeling in ROCK-I$^{+/-}$ROCK-II$^{-/-}$ and ROCK-I$^{-/-}$ROCK-II$^{+/-}$ yolk sacs at 9.5 dpc. Yolk sacs from 8.5 or 9.5 dpc embryos of indicated genotypes were stained with anti-Flk-1 antibody.

Whole-mount flat views (A, B, D and E) and slices sectioned along the transverse plane of Flk-1-stained yolk sacs were shown (C, F and G). (A, B, D and E) Bars, 250 μm. (C, F and G) Bars, 50 μm. Arrowheads in F and G show the blood cells.

Figure 4 Impairment of vascular remodeling and body turning in Y-27632 treated embryos in whole embryo culture system.

Impaired vascular remodeling and body turning of embryos cultured *ex vivo* in the presence of Y-27632. Embryos of 7.5 dpc were dissected and then cultured in rat serum at 37 ℃ under 5% O_2, 5% CO_2 and 90% N_2 for 24 h, followed by 20% O_2, 5% CO_2 and 75% N_2 for another 24 h in the presence or absence of indicated concentrations of Y-27632. At 48 h, the embryos were collected and photographs of dissected embryos with (A–C) or without (D–F) intact yolk sacs were taken. Bars, 500 μm. (G–I) Yolk sacs of embryos were sectioned along the transverse plane and

stained with hematoxylin–eosin. Bars, 250 μm.

Figure 5 Decreased phosphorylation of endogenous substrates for ROCK in yolk sacs of ROCK-I$^{+/-}$ROCK-II$^{-/-}$ and ROCK-I$^{-/-}$ROCK-II$^{+/-}$ embryos and embryos treated with Y-27632.

Yolk sacs were obtained from embryos of indicated genotypes and embryos cultured in the presence or absence of indicated concentrations of Y-27632 and lysed with Laemmli buffer. The lysates were subjected to SDS-PAGE and then analyzed by immunoblotting with antibodies to phospho- MYPT, phospho-MLC and b-actin.

Table 1 Genotypes of offspring obtained by cross-mating of ROCK-I$^{+/-}$ROCK-II$^{+/-}$ double heterozygous (DHT) mice

Cross	Total		No. of mice with Genotype								
		ROCK-I	+/+	+/+	+/+	+/-	+/-	+/-	-/-	-/-	-/-
		ROCK-II	+/+	+/-	-/-	+/+	+/-	-/-	+/+	+/-	-/-
♂ROCK DHT x♀ ROCK DHT											
Mendelian's ratio			1	2	1	2	4	2	1	2	1
9.5 dpc	136		9	19	13	20	46	12	4	13	0
12.5 dpc	84		14	18	6	13	31	0	2	0	0

Table 2 Genotypes of offspring obtained by IVF of ROCK-I$^{+/-}$ROCK-II$^{+/-}$ double heterozygous (DHT) mice

Cross	Total		No. of mice with Genotype								
		ROCK-I	+/+	+/+	+/+	+/-	+/-	+/-	-/-	-/-	-/-
		ROCK-II	+/+	+/-	-/-	+/+	+/-	-/-	+/+	+/-	-/-
♂ROCK DHT x♀ ROCK DHT											
Mendelian's ratio			1	2	1	2	4	2	1	2	1
3.5 dpc	65		5	7	5	7	16	8	6	5	6

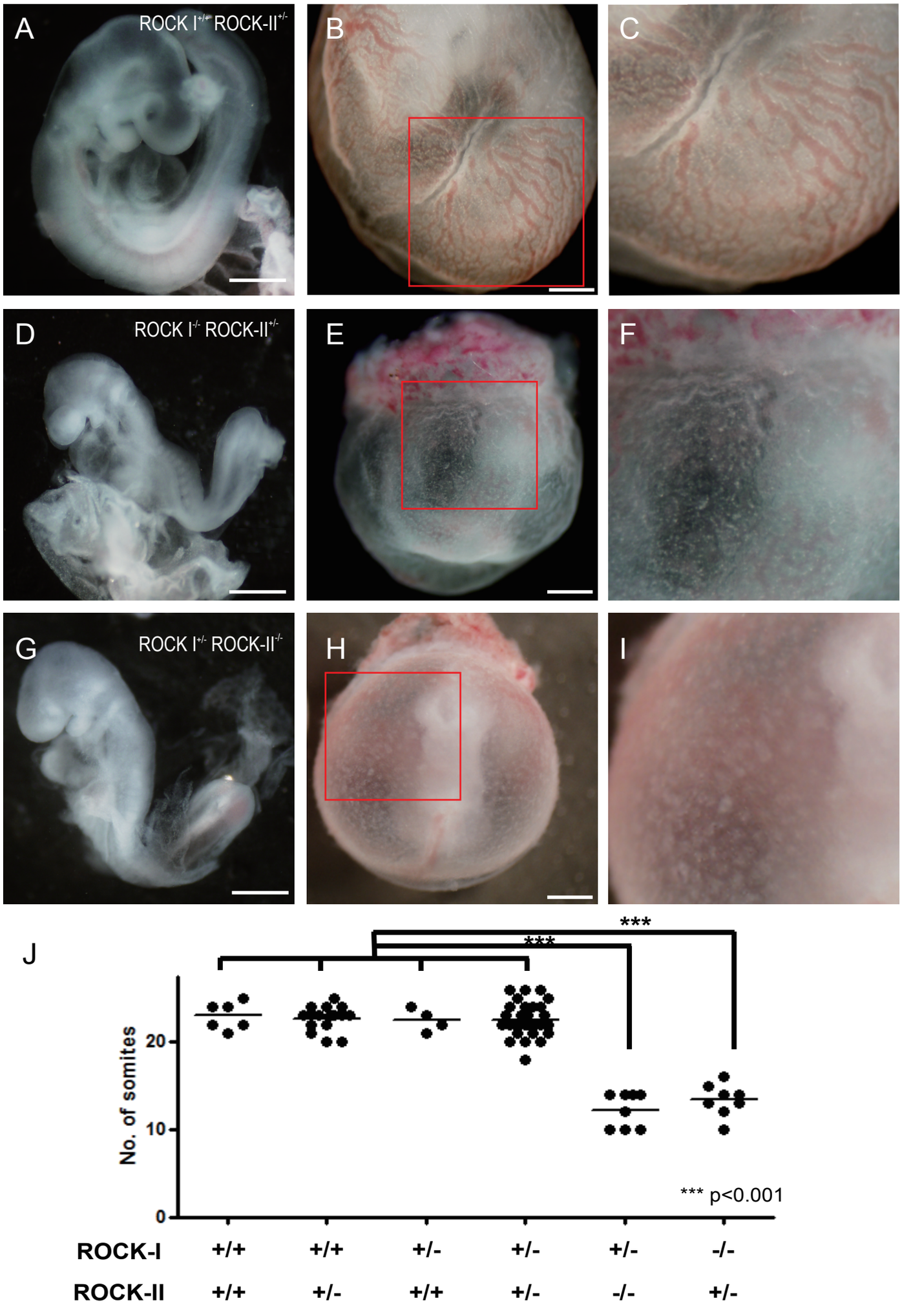

Figure 1 Kamijo et al.

A

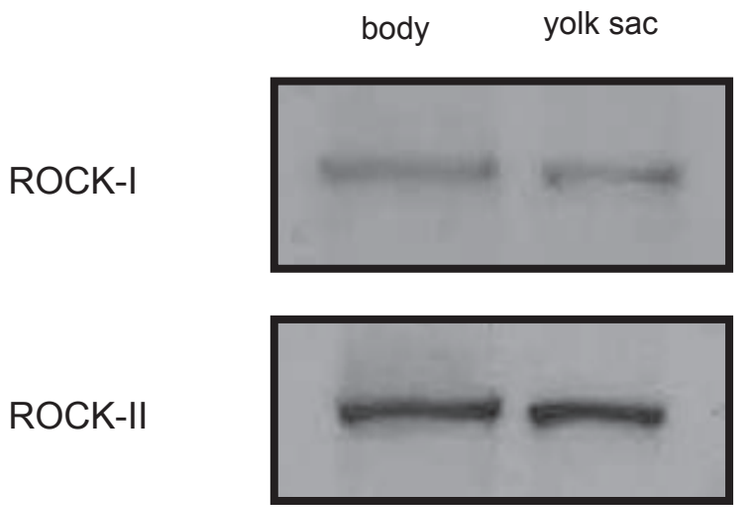

B

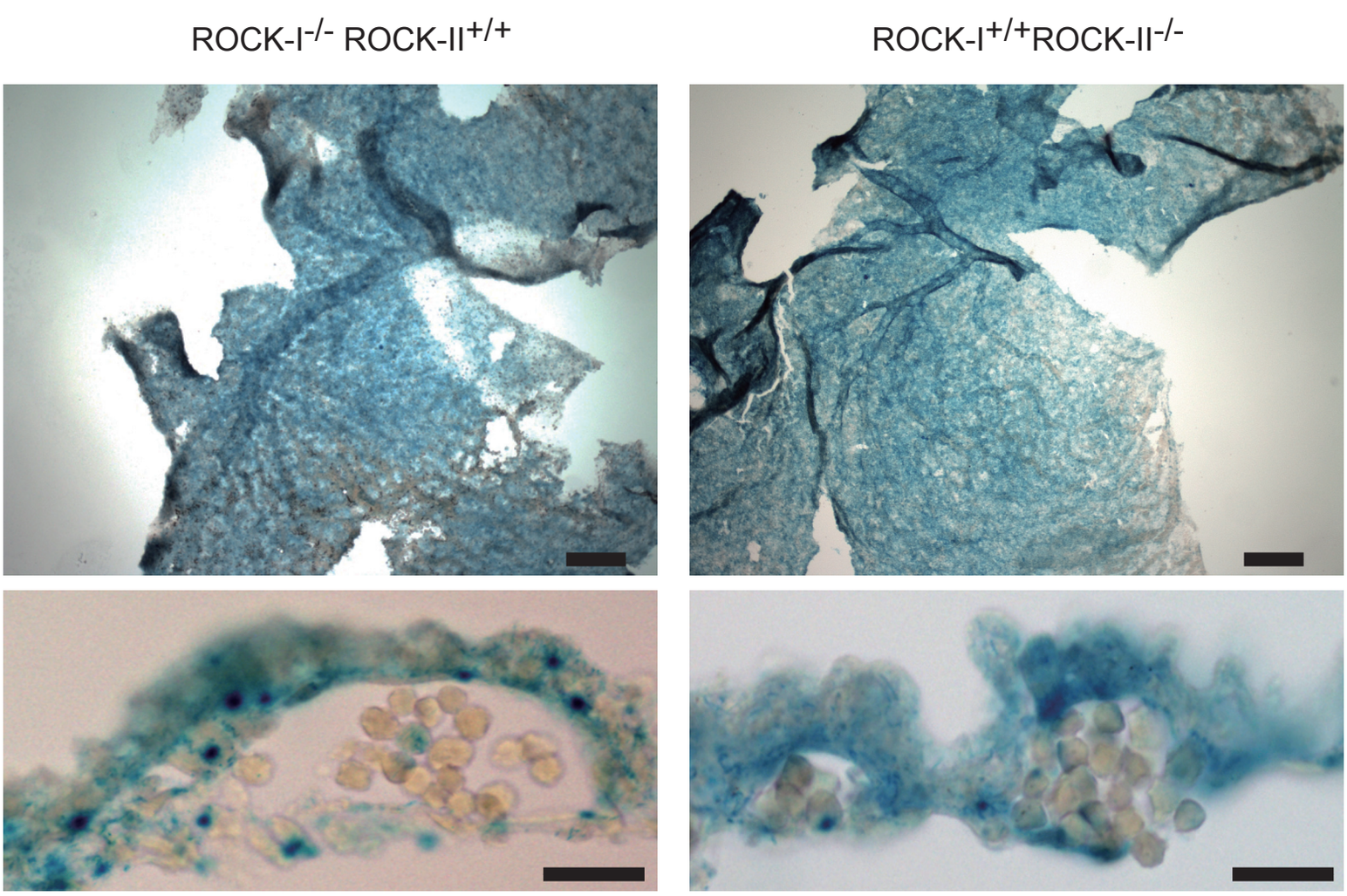

Figure 2 Kamijo et al.

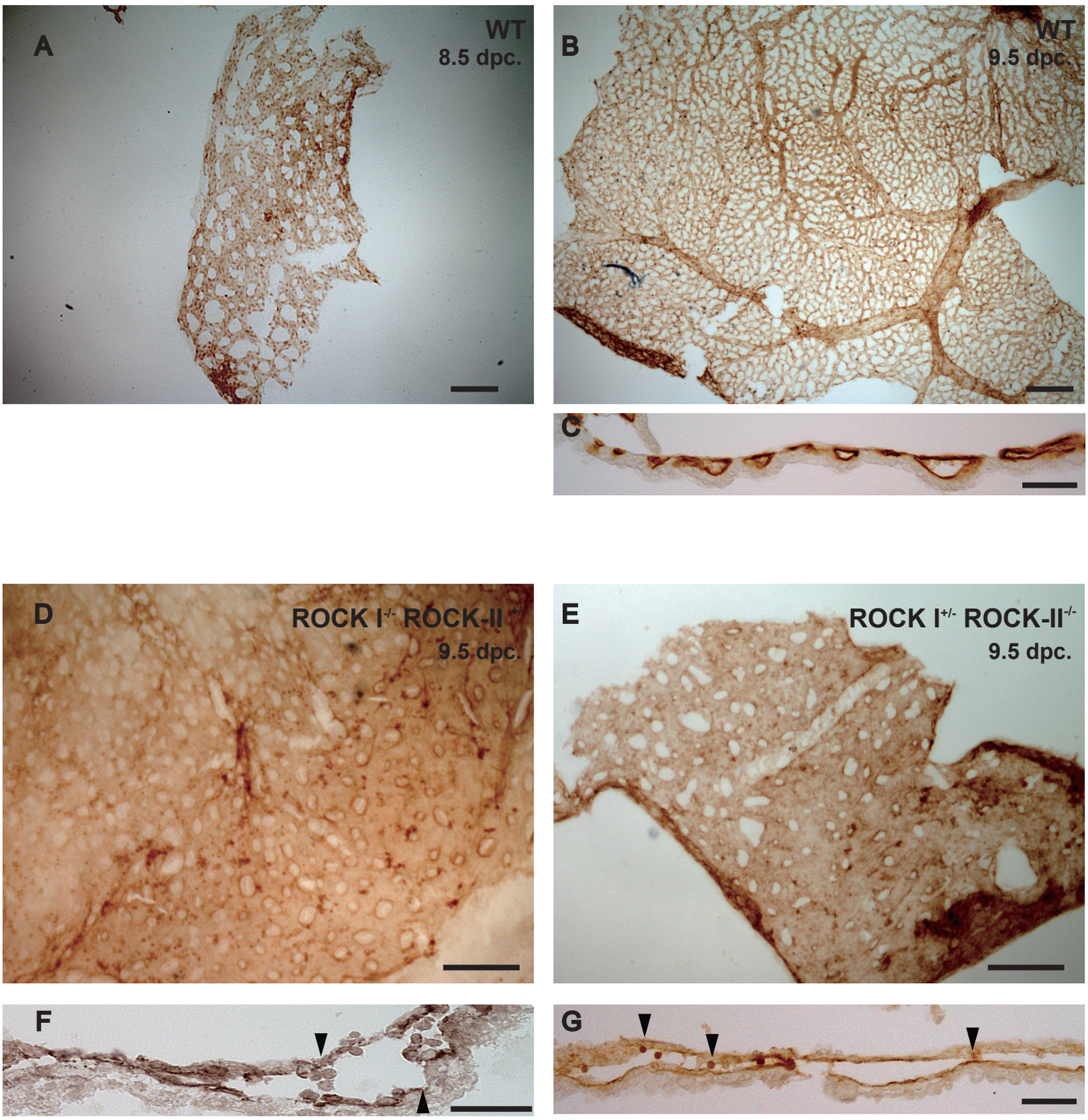

Figure 3 Kamijo et al.

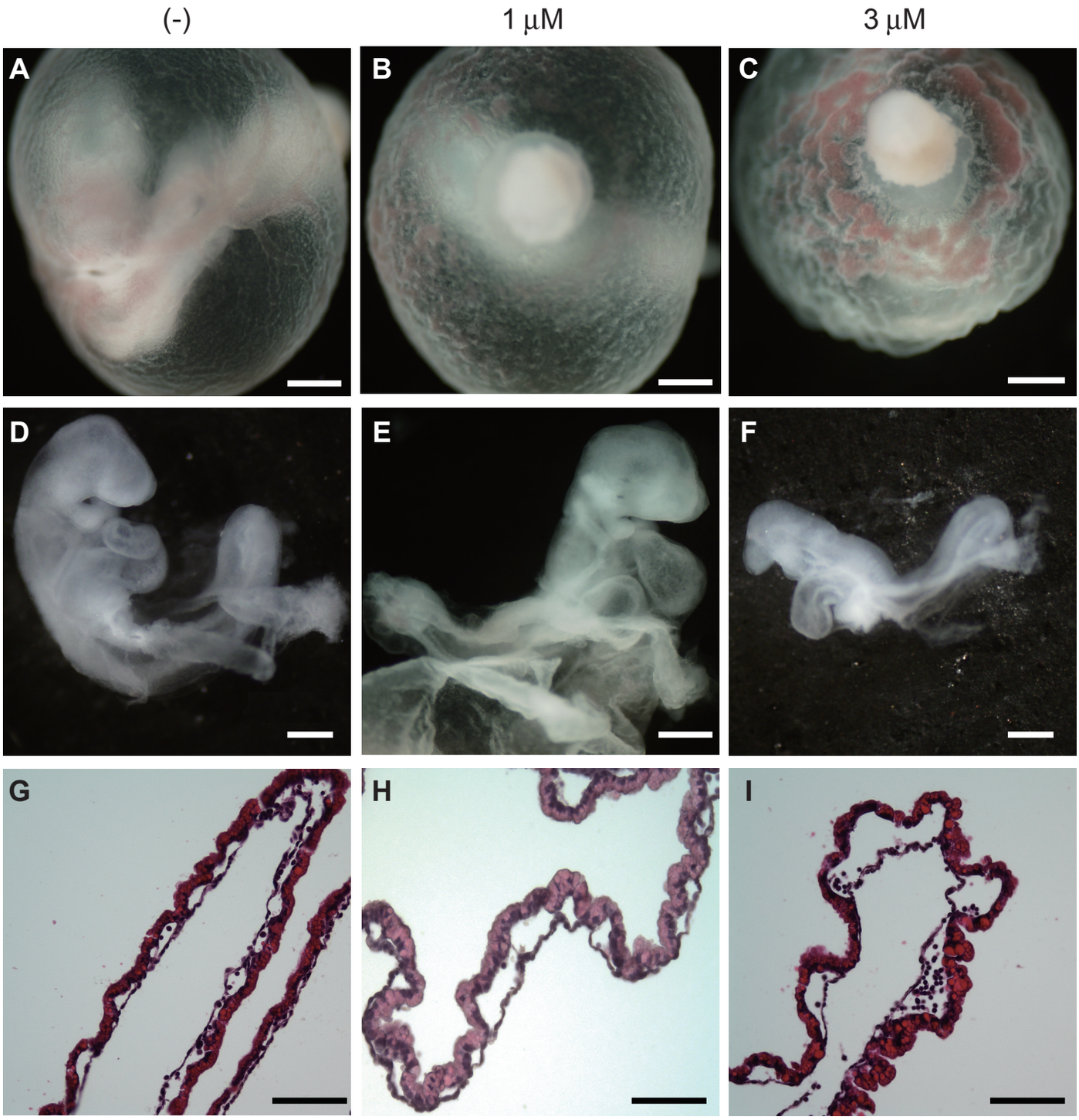

Figure 4 Kamijo et al.

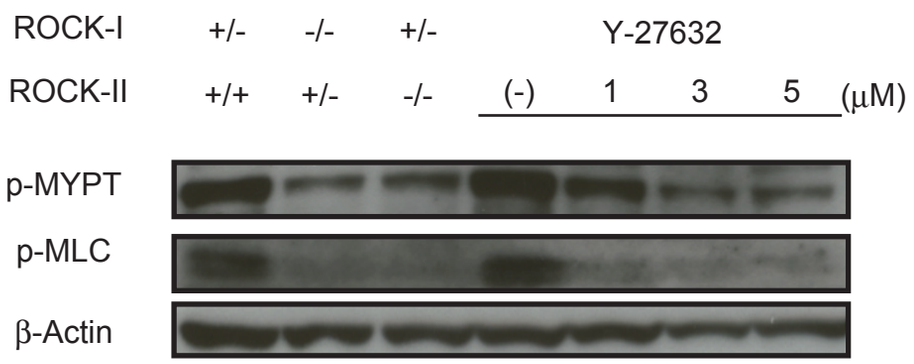

Figure 5 Kamijo et al.